

The GEM-Mars General Circulation Model for Mars: Description and Evaluation

L. Neary¹ and F. Daerden¹

¹Royal Belgian Institute for Space Aeronomy

Introduction:

Powerful and flexible atmospheric modeling capabilities are a vital and necessary tool in addition to an increasing observational dataset to enhance our understanding of the processes taking place in the Martian atmosphere.

The GEM-Mars three-dimensional general circulation model [1] takes advantage of the cutting edge efforts made by the numerical weather prediction (NWP) community by using the operational framework and dynamical core of the Global Environmental Multiscale (GEM) model from the Recherche en Prévision Numérique (RPN) division of Environment Canada [2][3][4]. The current version available to the community (under the GNU Lesser General Public Licence v2.1) is GEM 4.2.0 and this has been converted from the terrestrial application for the simulation of the Mars atmosphere. The advantage of using code from an operational weather prediction model is that it is fully parallelized and efficient.

The objective of this work is to present the current state and performance of the model now that the ESA-Roskosmos ExoMars Trace Gas Orbiter (TGO) mission is in orbit around Mars. GEM-Mars will play an integral part in the analysis of data that is received by the Nadir and Occultation for Mars Discovery (NOMAD) instrument [5] on board the TGO.

Model Description:

The dynamical core of GEM-Mars uses a semi-Lagrangian advection scheme with a two-time-level semi-implicit integration method that allows for a relatively long time step while maintaining stability. The option to run with hydrostatic or non-hydrostatic formulation of the primitive equations gives the capability of running at multiple horizontal scales down to the mesoscale. The results presented here will be at $4^\circ \times 4^\circ$ horizontal resolution, with 103 vertical levels up to ~ 160 km. The integration time step is 30 minutes.

The radiative transfer code in GEM-Mars includes CO_2 absorption and emission in the $15 \mu\text{m}$ band as given in [6] and absorption in the near infrared as described in [7]. For dust and water ice clouds, a two-stream method [8] is applied in 5 wavelength bands in the visible and infrared range. Dust is represented by 3 size bins (0.1 ,

1.5 and $10 \mu\text{m}$) and the spatiotemporal distribution is computed online with a dust lifting parameterization and transport due to advection, sedimentation and mixing. The dust optical depths can also be scaled to a climatological value [9] for a specific year. Figure 1 shows the zonal mean of dust optical depth at the equator computed by the model compared with the scaled climatological value for Mars year 26.

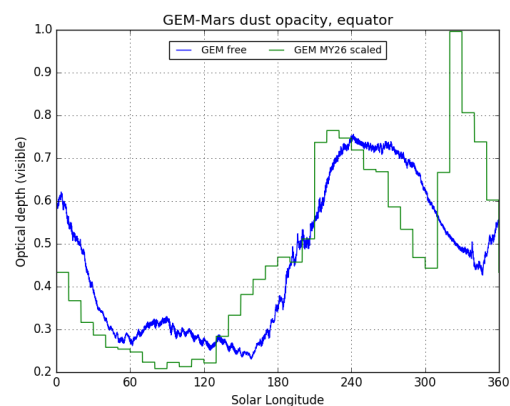


Figure 1 Equatorial zonal mean of dust optical depth for the free-running dust lifting scheme (blue) compared with the optical depths scaled to MY26 climatology (binned every $10 L_s$).

Water ice clouds are radiatively active, using the optical properties computed with refractive indices from [10] using $4 \mu\text{m}$ particles. As the model extends above 100 km, non-LTE corrections are applied [11].

The model also includes an interactive CO_2 condensation and surface pressure cycle, a thermal soil model, turbulent transport in the atmospheric surface layer and convective transport inside the planetary boundary layer. The effects of the extreme Martian topography are considered with a low level blocking scheme [12] and a gravity wave drag parameterization [13].

The model includes 15 chemical species with 15 photochemical and 31 gas-phase reactions. For methane experiments, a large number of tracers can be added.

Comparisons to Observations:

To evaluate the GEM-Mars GCM performance, we compare a generic one-year simulation with

free-running dust to observational datasets. Figure 2 shows the zonal mean total column H_2O vapour for one year compared to the average values measured by the Thermal Emission Spectrometer (TES) [14] onboard the Mars Global Surveyor (MGS). The model reproduces the main characteristics of the seasonal evolution.

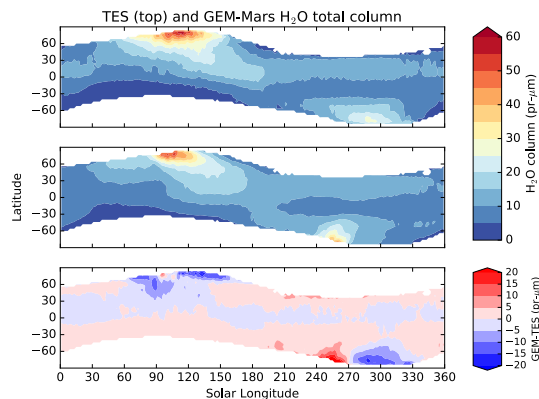


Figure 2 Zonal mean TES (top) column water vapour in $\text{pr-}\mu\text{m}$ compared with GEM-Mars (middle) with the difference in the lowest field.

To evaluate the gas-phase chemistry in the model, we use measurements by the Mars Color Imager (MARCI) [15] of column ozone. The major seasonal features are captured, including the maximums seen at high latitudes in fall, winter and spring.

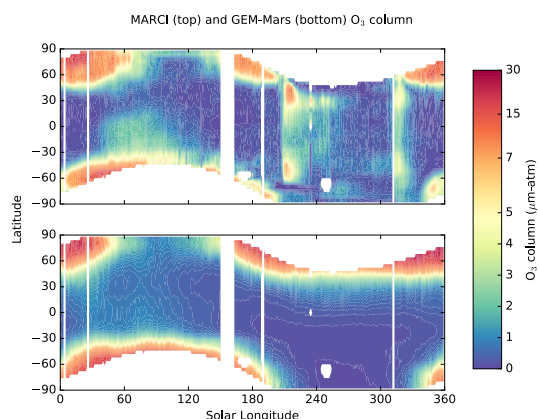


Figure 3 MARCI (top) zonal mean daytime column ozone compared with GEM-Mars (bottom).

Summary and Conclusions:

The BIRA-IASB GEM-Mars model has undergone significant updates and improvements and is positioned to play a vital role in the analysis of new data anticipated from the NOMAD instrument on the ExoMars TGO mission. We describe the fundamentals of the model, its capa-

bilities and evaluate the main atmospheric fields by comparing to the latest data.

Recently the model has been applied to uniquely explain detached layers of dust in the northern summer that were observed by the Phoenix lander [16]. Also the transport and vertical distribution of methane after a surface release was investigated with the model [17]. The climatology of CO and H_2O from the model was compared with observations from the Compact Reconnaissance Imaging Spectrometer for Mars (CRISM) [18].

References:

- [1] Neary, L. and Daerden, F., *Icarus* 300, 458-476, 2017.
- [2] Côté et al., *Mon. Wea. Rev.*, 126(6), 1373-1395, 1998a.
- [3] Côté et al., *Mon. Wea. Rev.*, 126(6), 1397-1418, 1998b.
- [4] Yeh et al., *Mon. Wea. Rev.*, 130, 339-356, 2002.
- [5] Vandaele et al., *Planet. Space Sci.*, 119, 233-249, 2015.
- [6] Hourdin, F., *J. Geophys. Res.*, 97 (E11), 18,319-18,335, 1992.
- [7] Forget et al., *J. Geophys. Res.*, 104 (E10), 24,155-24,175, 1999.
- [8] Toon et al., *J. Geophys. Res.*, 94 (D13), 16,287-16,301, 1989.
- [9] Montabone et al., *Icarus*, 251, 65-95, 2015.
- [10] Warren S.G. and Brandt, R.E., *J. Geophys. Res.*, 113, D14220, 2008.
- [11] Lopez-Valverde et al., *J. Geophys. Res.*, 99(E6), 13,093-13,115, 1994.
- [12] Zadra et al., *Atmos.-Ocean*, 41 (2), 155-170, 2003.
- [13] McFarlane, N.A., *J. Atmos. Sci.*, 44 (14), 1775-1800, 1987.
- [14] Smith et al., *Icarus*, 167, 148-165, 2004.
- [15] Clancy et al., *Icarus*, 266, 122-133, 2016.
- [16] Daerden et al., *Geophys. Res. Lett.*, 42, 73197326, 2015
- [17] Viscardy et al., *Geophys. Res. Lett.*, 43(5), 1868-1875, 2016
- [18] Smith et al., *Icarus*, 2017.

Acknowledgements:

The research leading to these results has received funding from the European Community's Seventh Framework Programme (FP7/2007-2013) under grant agreement no. 607177 CrossDrive and from the ESA PRODEX Office 0121493_2017-2019).